Title:

Sensitivity enhancement of laser absorption spectroscopy for atomic oxygen measurement in microwave air plasma

Authors:

Makoto Matsui [a] *, Kimiya Komurasaki [b] and Yoshihiro Arakawa [a]

Affiliations:

[a] Department of Aeronautics and Astronautics, The University of Tokyo

7-3-1 Hongo, Bunkyo, Tokyo 113-8656, Japan

[b] Department of Advanced Energy, The University of Tokyo

5-1-5 Kashiwanoha, Kashiwa, Chiba 277-8561, Japan

Corresponding Author:

Makoto Matsui

Department of Aeronautics and Astronautics,

The University of Tokyo

5-1-5 Kashiwanoha,

Kashiwa, Chiba 277-8561, Japan

Fax: +81-4-7136-4030

Email: matsui@al.t.u-tokyo.ac.jp

Abstract:

A high sensitive laser absorption spectroscopy system has been developed for the detection of atomic oxygen in a microwave plasma. Firstly, the sensitivity of this system was evaluated by ring-down time measurement. The effective absorbing pass length was extended up to 640 times as long as that of the conventional laser absorption spectroscopy. Then, the system was applied to the air plasma diagnostics. As a result, the absorption signal from the meta-stable atomic oxygen at 777.19 nm could be observed at the input enthalpy range from 0.93 MJ/kg to 467 MJ/kg. The detected minimum number density was 1.6×10^{11} m^{-3} with temperature of 388 K, which correspond to the center fractional absorption of 1.4×10^{-2} % in the LAS.

Keywords:

Atomic Oxygen, Air Plasma, Microwave Plasma, High Sensitive Laser Absorption Spectroscopy

1. Introduction

Air plasma has been used in various research fields such as welding and cutting [1], waste disposal of hazardous material [2], plasma etching for semiconductor [3] and developments of thermal protection system for re-entry vehicles [4]. Although various

plasma devices such as microwave, radio frequency, and arc plasmas have been developed to produce air plasma, their properties are difficult to characterize because they are usually in strong thermo-chemical non-equilibrium.

In our previous studies, laser absorption spectroscopy (LAS) was applied to various plasma devices [5-10]. The results showed that strong absorption signals from the meta-stable atomic oxygen OI (3s5S) at 777.19 nm line were observed in argon/oxygen or pure oxygen flows and the OI (3s5S) number density and the translational temperature were successfully measured. However, in nitrogen/oxygen or air flows, the fractional absorption was as much as or smaller than the detectable limit of 1 %. This might be because the excitation temperature was lower than that of the argon/oxygen flow due to the nitrogen dissociation, resulting in the lower number density of OI (3s5S). Fig. 1 shows the calculated translational temperature, degree of dissociation in oxygen and OI (3s5S) fraction of total atomic oxygen in argon/oxygen and air plasma for a typical input specific enthalpy range. Here, for simplicity, thermo-chemical equilibrium and Boltzmann relation between the ground and the meta-stable are assumed. The figure shows OI (3s5S) in the nitrogen/oxygen flow is two orders of magnitude smaller than that of the air flow due to the lower temperature even if the oxygen is fully dissociated. Then, sensitivity enhancement of conventional LAS is necessary to measure OI (3s5S)

absorption in nitrogen/oxygen or air flows. In this study, a high sensitive laser absorption spectroscopy system has been developed using integrated cavity output spectroscopy (ICOS) [11-13]. In addition to advantages of the LAS, the ICOS is simpler and more robust system than other high sensitive LAS such as cavity ring down spectroscopy or cavity enhanced spectroscopy [14-16].

This paper describes sensitivity enhancement of the system evaluated by ring-down time measurement and applicable limit for OI (3s5S) detection in microwave air plasma.

2. Experimental procedure

2.1 Principle of ICOS

The fractional absorption of the laser intensity $\Delta I/I_0$ is related to the absorption coefficient k by the Beer-Lambert law expressed as,

$$\left(\frac{\Delta I}{I_0}\right)_{\mathrm{LAS}} = \frac{I_0 - I_t}{I_0} = 1 - \exp\left(kd_0\right). \tag{1}$$

Here, I_0, I_t and d_0 are the incident and the transmitted laser intensity and the absorbing pass length, respectively.

In the ICOS, the integrated laser intensity leaking out from the cavity is expressed as,

$$\left(\frac{\Delta I}{I_0}\right)_{\mathrm{ICOS}} = 1 - \exp\left(-kd_{\mathrm{ICOS}}\right) = \frac{R_{\mathrm{eff}}\left\{1 - \exp\left(-kd_0\right)\right\}}{1 - R_{\mathrm{eff}} \cdot \exp\left(-kd_0\right)}. \tag{2}$$

If $kd_0 << 1$, the effective pass ratio is approximated as,

$$\frac{d_{\mathrm{ICOS}}}{d_0} \approx \frac{R_{\mathrm{eff}}}{1-R_{\mathrm{eff}}}. \tag{3}$$

Here, d_{ICOS} and R_{eff} are the effective absorbing pass length in the ICOS and the effective mirror reflectance, respectively. Fig. 2 shows the relationship between $(\Delta I/I_0)_{\mathrm{LAS}}$ and the absorbing pass ratio d_{ICOS}/d_0 for several mirror reflectance. This figure shows the absorbing pass ratio increases with the decrease in the fractional absorption in the LAS and Eq.(3) exhibits the maximum absorbing pass ratio under the system with R_{eff}.

The effective mirror reflectance is estimated by the ring-down time. When the laser beam was switched off, the laser intensity leaking out from the cavity $I(t)$ has a time variation expressed as,

$$I(t) = I_0 \exp(-t/\tau) \tag{4}$$

,where τ is called ring-down time and defined as,

$$\tau = \frac{L}{c(1-R_{\mathrm{eff}})}. \tag{5}$$

Here, t, L, c are the elapsed time, the cavity length and the velocity of light, respectively.

In our experimental conditions, Doppler broadening is several gigahertzes, which is two orders of magnitude greater than all other broadenings. The absorption profile k at laser frequency ν is approximated as a Gaussian profile, expressed as,

$$k(\nu) = \frac{2K}{\Delta\nu_{\mathrm{D}}}\sqrt{\frac{\ln 2}{\pi}}\exp\left\{-\ln 2\left[\frac{2(\nu-\nu_0)}{\Delta\nu_{\mathrm{D}}}\right]^2\right\}. \quad (6)$$

Here, ν_0 and K are the center absorption frequency and the integrated absorption coefficient, respectively. $\Delta\nu_{\mathrm{D}}$ is the full width at half maximum of the profile and is related to the translational temperature T, expressed as,

$$\Delta\nu_{\mathrm{D}} = 2\nu_0\sqrt{\frac{2\ln 2 k_{\mathrm{B}}T}{mc^2}} \quad (7)$$

,where m and k_{B} represent the mass of absorbers and the Boltzmann constant, respectively.

The number density of absorbers n_i is related to K as,

$$n_i = \frac{8\pi\nu_0^2}{c^2 A_{ji}}\frac{g_i}{g_j}K. \quad (8)$$

Here, A_{ji} is the Einstein coefficient, g is the statistical weight and i, j shows absorbing and excited states, respectively.

2.2 Experimental apparatus

Fig. 3 shows a schematic of the measurement system. A tunable diode-laser with an external cavity (Velocity Model 6300; New Focus Inc.) was used as the laser oscillator. Its line width was less than 300 kHz. The laser beam was guided to the microwave discharge tube through an optical fiber. At both sides of the tube, high reflection concave mirrors (HR820; Layertec) whose curvature radius were 1 m were equipped to form an optical cavity. The cavity length was 0.97 m and corresponding free spectral

range was 155 MHz. The fiber output was mounted on a collimate lens and the probe beam was led into the cavity with an off-axis mode.

In the ring-down time measurement, an acousto-optic modulator (AOM 1205C; ISOMET Co.) was set in front of the fiber coupler to switch off the laser beam within the rise time of 200 ns. The ring-down time was recorded using a high speed digital oscilloscope (DL1540; Yokogawa Co.) with 8-bit resolution and the bandwidth of 150 MHz.

In the ICOS measurement, the laser frequency was scanned over the absorption line shape. The modulation frequency and width were 1 Hz and 30 GHz, respectively. An optical isolator was used to prevent the reflected laser beam from returning into the external cavity. An etalon was used as a wave-meter. Its free spectral range was 0.75 GHz. The transmitted laser intensity was focused on a photo multiplier tube (H7732; Hamamatsu) with a band pass filter (FB780-10; Thorlab, Inc.) and a preamplifier (C9663; Hamamatsu). Signals were recorded using a digital oscilloscope (DL708E; Yokogawa Co.) with 14-bit resolution and a 500 Hz low pass filter.

In this study, secondary modulation was applied to suppress the fluctuation of the transmitted laser intensity as well as the profile scanning. This modulation frequency and width were 1 MHz and 100 MHz, respectively. Fig. 4 shows transmitted laser

intensity with and without the modulation. The fluctuation of 20% was successfully reduced less than 1 % by the modulation.

3. Results and discussion

3.1 Ring-down time measurement

Fig. 5 shows a decay signal of the transmitted laser intensity and a curve fit of Eq.(4) before and after the laser beam was switched off by the AOM. From the measured ring-down time, the effective mirror reflectance was estimated at 0.9984. Then, in this system, the effective absorbing pass length was extended up to 640 times as long as that of the LAS.

3.2 Air flow diagnostics

Next, the air plasma generated by the microwave discharge tube was diagnosed by the ICOS system. The input specific enthalpy was changed from 0.47 MJ/kg to 467 MJ/kg by the variation of the mass flow from 10 sccm to 10 slm with the fixed input power of 100 W. The corresponding ambient pressure was ranged from 24 Pa to 186 Pa.

Fig. 6 shows typical transmitted laser intensity and etalon signals at the input enthalpy of 4.7 MJ/kg. Strong absorption signal was observed though in this condition no absorption signal could be detected by the LAS.

Fig. 7 shows the corresponding fractional absorption and a curve fit of Eqs. (2) and (6), where measured R_{eff} was used. The deduced center absorption coefficient was 3.5×10^{-3} m^{-1}, which corresponds to the fractional absorption of 0.34 % in the LAS. The OI (3s5S) number density and the translational temperature were estimated at 4.8×10^{12} m^{-3} and 521 K, respectively. Fig. 7 also shows the effective absorbing pass ratio in the profile. At the center absorption frequency, the ratio decreased to 339 due to the relatively large fractional absorption as seen in Fig.2. This is because the measured profile shows the saturation around the center absorption frequency.

Fig. 8 shows measured OI (3s5S) number density and temperature as a function of input specific enthalpy. The absorption signal could be detected at the input specific enthalpy more than 0.93 MJ/kg. Both number density and temperature rapidly increases until the input specific enthalpy of 10 MJ/kg and then they are almost independent of it. The detected minimum number density was $1.6\times10^{11}m^{-3}$ with the temperature of 388K. This value corresponds to the center fractional absorption of 1.4×10^{-2} % in the LAS.

4. Conclusion

(1) A high sensitive laser absorption spectroscopy system has been developed using integrated cavity output spectroscopy.

(2) The sensitivity of this system was evaluated by measuring the ring-down time. The maximum effective absorbing pass length was extended up to 640 as long as that of the LAS.

(3) As a result of the air plasma diagnostics in the microwave discharge tube, the absorption signals of the meta-stable atomic oxygen at 777.19 nm line were successfully detected in the input specific enthalpy range from 0.93 MJ/kg to 467 MJ/kg.

(4) The detected minimum number density of OI (3s5S) was $1.6\times10^{11}m^{-3}$ at temperature of 388K, which correspond to the center fractional absorption of 1.4×10^{-2} % in the LAS.

Acknowledgements

This research was partially supported by Research Fellowships of the Japan Society for the Promotion of Science for Young Scientists 18-09885.

References

[1] Pardo C, Gonzalez-Aguilar J, Rodriguez-Yunta A, Calderon MAG. J Phys D: Appl Phys 1999;32: 2181.

[2] Suzuki M, Komatsubara M, Umebayashi M, Akatsuka H. J Nucl Sci Technol 1997;34:1159.

[3] Martinez H, Rodriguez-Lazcano Y, Castillo F. Plasma Sources Sci Technol 2007; 16:427.

[4] Auweter-Kurtz M. NATO Research and Technology Organization proceedings 2000; RTO-EN-8: p.2A1-2A-20.

[5] Matsui M, Takayanagi H, Oda Y, Komurasaki K, Arakawa Y. Vacuum 2004; 73, 3-4:341.

[6] Matsui M, Komurasaki K, Herdrich G, Auweter-Kurtz M. AIAA J 2005;43:2060.

[7] Yamamoto Y, Yokota S, Matsui M, Komurasaki K, Arakawa Y. Rev Sci Instrum 2005; 76:083111.

[8] Inoue T, Matsui M, Takayanagi H, Komurasaki K, Arakawa Y. Vacuum 2006; 80:1174.

[9] Matsui M, Ogawa S, Komurasaki K, Arakawa Y. J Appl Phys 2006;100:063102.

[10] Matsui M, Ikemoto T, Takayanagi H, Komurasaki K Arakawa Y. J Thermophys

Heat Tr 2007; 21:247.

[11] Paul JB, Lapson L, Anderson JG. Appl Opt 2001;40:4904.

[12] Baer DS, Paul JB, Gupta M, O'Keefe A. Appl Phys B 2002;75:261.

[13] Gupta M, Owano T, Baer DS, O'Keefe A. Chem Phys Lett 2006;418:11.

[14] O'Keefe A, Deacon DAG. Rev Sci Instrum 1988;59:2544.

[15] Gianfrani L, Fox RW, Hollberg L. J Opt Soc Am B 1999;16:2247.

[16] Paldus BA, Kachanov AA. Can J Phys 2005;83:975.

Figure Captions:

Fig. 1 Calculated temperature, degree of dissociation in oxygen and OI (3s5S) mole fraction of total atomic oxygen in air and argon/oxygen (volumetric mixture ratio Ar: O_2=4:1) using the thermo-chemical equilibrium assumption, p_0=100 kPa.

Fig. 2 Absorbing pass ratio as a function of fractional absorption in the LAS and effective mirror reflectance.

Fig. 3 Measurement system.

Fig. 4 Transmitted laser intensity with and without secondary modulation.

Fig. 5 Ring-downtime and curve fit of Eq.(4).

Fig. 6 Transmitted laser intensity and etalon signals.

Fig. 7 Measured fractional absorption, curve fit and effective absorbing pass ratio.

Fig. 8 Measured number density and temperature as a function of input specific enthalpy.

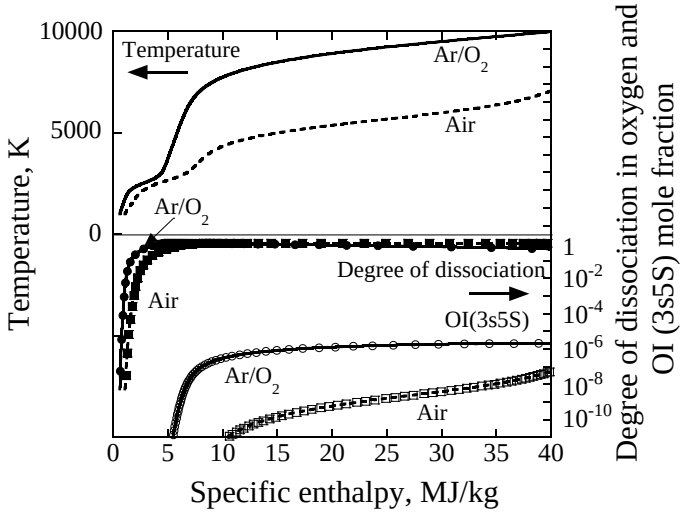
10000
5000
0
Temperature
Ar/O2
Air
Ar/O2
Air
Degree of dissociation
OI(3s5S)
Ar/O2
Air
1
10-2
10-4
10-6
10-8
10-10
0
5
10
15
20
25
30
35
40
Temperature, K
Specific enthalpy, MJ/kg
Degree of dissociation in oxygen and
OI (3s5S) mole fraction

Fig. 1 (100%)

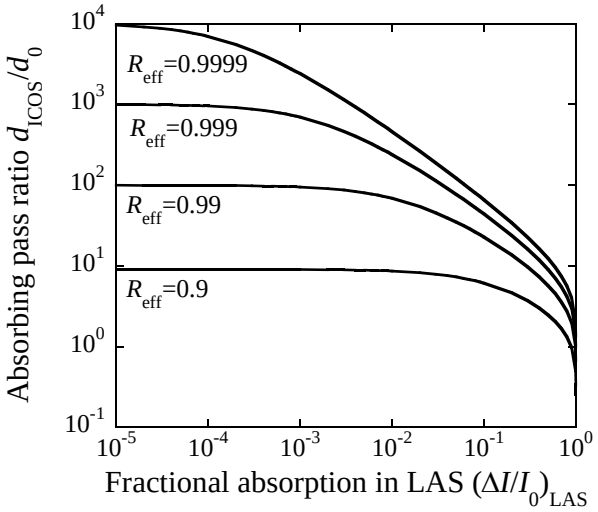
Absorbing pass ratio d_{ICOS}/d_0
10^4
10^3
10^2
10^1
10^0
10^{-1}
R_{eff}=0.9999
R_{eff}=0.999
R_{eff}=0.99
R_{eff}=0.9
10^{-5}
10^{-4}
10^{-3}
10^{-2}
10^{-1}
10^0
Fractional absorption in LAS $(\Delta I/I_0)_{LAS}$

Fig. 2 (100%)

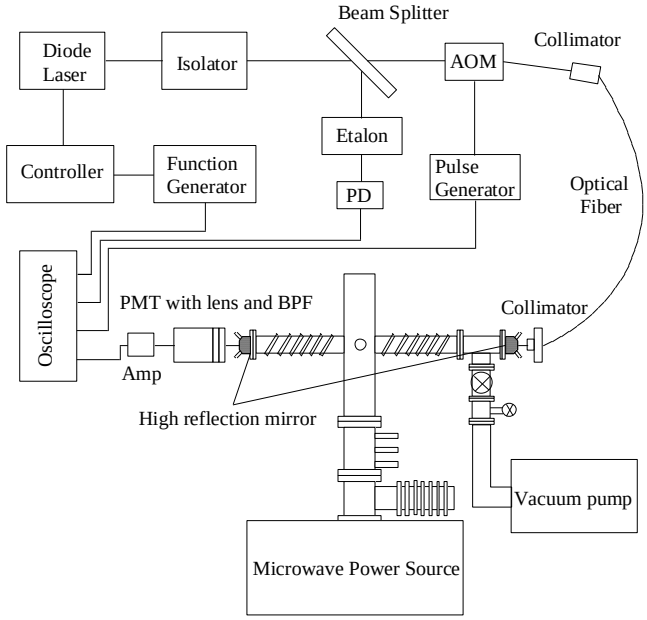
Beam Splitter
Diode Laser
Isolator
AOM
Collimator
Etalon
Controller
Function Generator
PD
Pulse Generator
Optical Fiber
Oscilloscope
PMT with lens and BPF
Collimator
Amp
High reflection mirror
Vacuum pump
Microwave Power Source

Fig. 3 (100%)

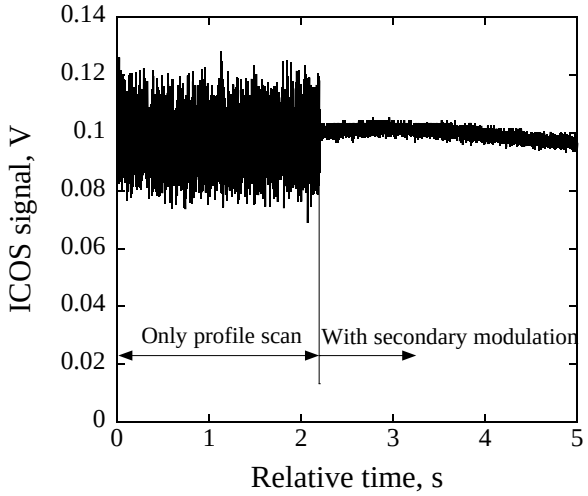
0.14
0.12
0.1
0.08
0.06
0.04
0.02
0
ICOS signal, V
Only profile scan
With secondary modulation
0
1
2
3
4
5
Relative time, s

Fig. 4 (100%)

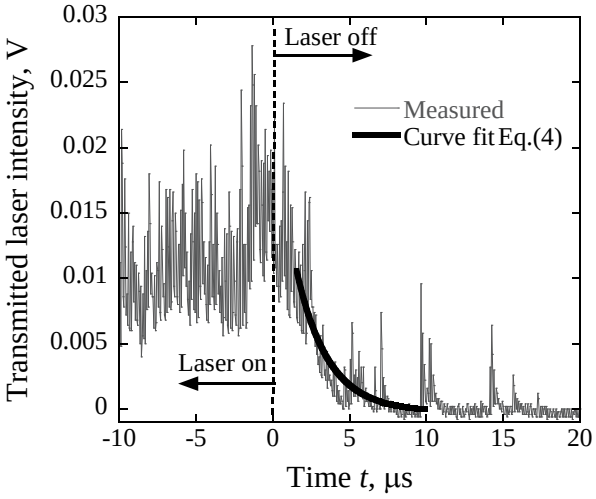
Transmitted laser intensity, V
0.03
0.025
0.02
0.015
0.01
0.005
0
-10
-5
0
5
10
15
20
Time t, μs
Laser off
Laser on
Measured
Curve fit Eq.(4)

Fig. 5 (100%)

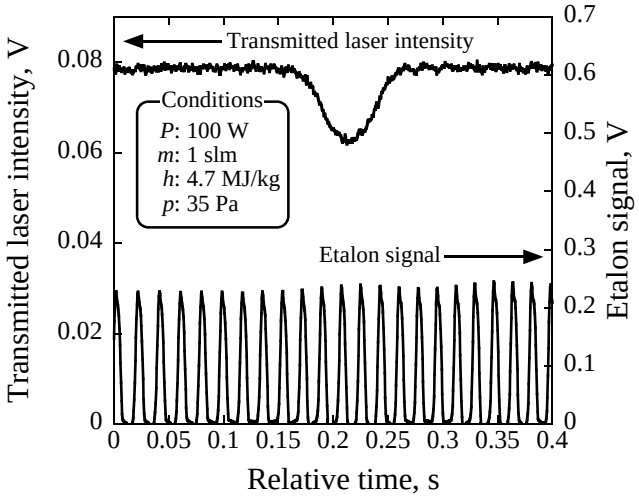
Transmitted laser intensity
Conditions
P: 100 W
m: 1 slm
h: 4.7 MJ/kg
p: 35 Pa
Etalon signal
Transmitted laser intensity, V
Etalon signal, V
Relative time, s
0
0.02
0.04
0.06
0.08
0.1
0.2
0.3
0.4
0.5
0.6
0.7
0.05
0.15
0.25
0.35

Fig. 6 (100%)

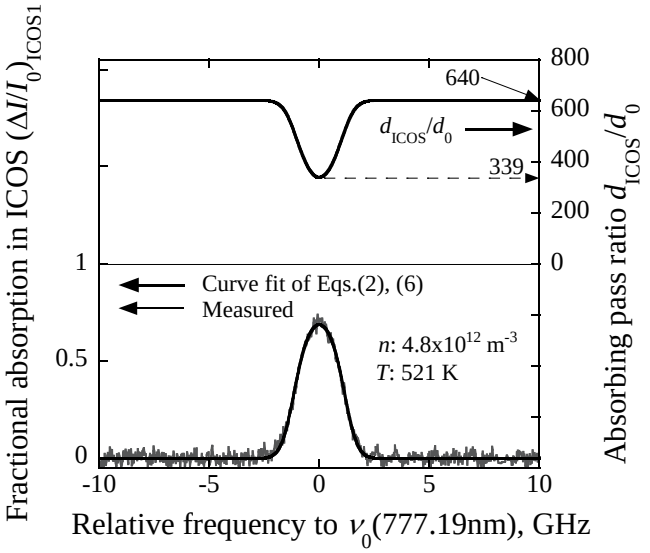
Fractional absorption in ICOS $(\Delta I/I_0)_{ICOS1}$
Absorbing pass ratio d_{ICOS}/d_0
640
339
d_{ICOS}/d_0
Curve fit of Eqs.(2), (6)
Measured
n: 4.8x10^{12} m^{-3}
T: 521 K
800
600
400
200
0
1
0.5
0
-10
-5
0
5
10
Relative frequency to ν_0(777.19nm), GHz

Fig. 7 (100%)

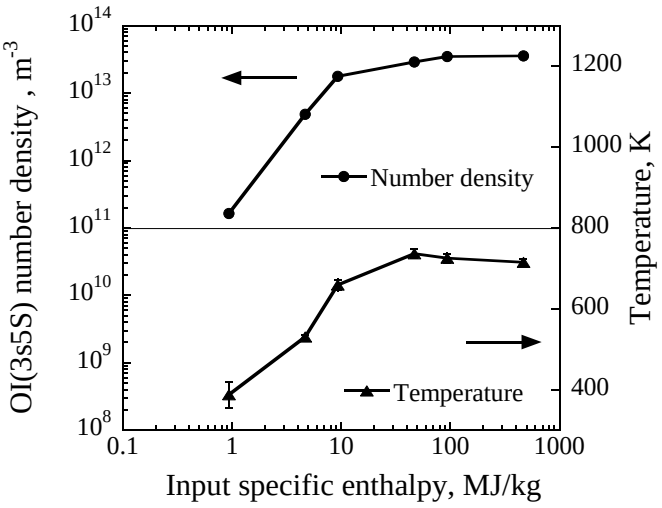
OI(3s5S) number density , m-3
Temperature, K
Number density
Temperature
Input specific enthalpy, MJ/kg

Fig. 8 (100%)